NUMERICAL INVESTIGATION OF NATURAL CONVECTION HEAT TRANSFER IN A SYMMETRICALLY COOLED SQUARE CAVITY WITH A THIN FIN ON ITS BOTTOM WALL

by

Saeid JANI [a], Mostafa MAHMOODI [b], Meysam AMINI [c], and Jafar E. JAM [d]*

[a] Department of Mechanical Engineering, Golpayegan College of Engineering, Golpayegan, Iran
[b] Mechanical Engineering Department, Amirkabir University of Technology, Tehran, Iran
[c] Department of Mechanical Engineering, University of Kashan, Kashan, Iran
[d] Composite Materials and Technology Center, Tehran, Iran

In the present paper, natural convection fluid flow and heat transfer in a square cavity heated from below and cooled from sides and the ceiling with a thin fin attached to its hot bottom wall is investigated numerically. The right and the left walls of the cavity, as well as its horizontal top wall are maintained at a constant temperature T_c, while the bottom wall is kept at a constant temperature T_h, with $T_h > T_c$. The governing equations are solved numerically using the finite volume method and the couple between the velocity and pressure fields is done using the SIMPLER algorithm. A parametric study is performed and the effects of the Rayleigh number and the length of the fin on the flow pattern and heat transfer inside the cavity are investigated. Two competing mechanisms that are responsible for the flow and thermal modifications are observed. One is the resistance effect of the fin due to the friction losses which directly depends on the length of the fin, whereas the other is due to the extra heating of the fluid that is offered by the fin. It is shown that for high Rayleigh numbers, placing a hot fin at the middle of the bottom wall has more remarkable effect on the flow field and heat transfer inside the cavity.

Key words: *natural convection, numerical simulation, square cavity, thin fin*

Introduction

Free convection heat transfer occurs in many industrial and engineering systems such as solar collectors, home ventilation systems, refrigeration unit, fire prevention, *etc*. [1]. In general, increasing, controlling, and modification of fluid flow and heat transfer inside the differentially heated cavities is down using a partition or fin attached to the walls. Many researchers have been investigated free convection inside cavities with fin on the walls. Zimmerman and Acharya [2] conducted a numerical study on free convection heat transfer in a cavity with a centrally mounted vertical finitely conducting baffle to one-half of the cavity height and attached to the floor or ceiling. They found that the baffle strongly influences the hot-wall Nusselt number distribution, but has a weaker effect on the cold-wall Nusselt number distribution. Frederick [3]

---

* Corresponding author: e-mail: parssystemenergy@yahoo.com

studied numerically laminar free convection in an air filled differentially heated inclined cavities with a thin partition placed at the middle of its cold wall. Frederick and Valencia [4] studied free convection heat transfer in a square cavity with a conducting partition located at the middle of its hot wall using a numerical simulation. They observed that for a low value of the partition-to-fluid thermal conductivity ratio and for Rayleigh numbers 10^4-10^5 a reduction in heat transfer relative to the case of cavity with no partition occurs. Nag *et al.* [5] investigated the effect of a horizontal thin partition positioned on the hot wall of a horizontal square cavity. They observed that for a partition of infinity thermal conductivity, the Nusselt number on the cold wall is greater than the case with no fin. Lakhal *et al.* [6] studied numerically natural convection in inclined rectangular cavities with perfectly conducting fins attached on the heated wall. Bilgen [7] reported numerical results of laminar and turbulent free convection in cavities with partition positioned on the insulated horizontal walls. Results of a numerical study on laminar free convection in a differentially heated square cavity due to a perfectly conducting thin fin on its hot wall were reported by Shi and Khodadadi [8]. They found that heat transfer on the cold wall without fin can be promoted for high Rayleigh numbers and with the fins placed closer to the insulated walls. Effect of radial fins on turbulent natural convection in a horizontal annulus was investigated by Rahnama and Farhadi [9], numerically. Results obtained for local Nusselt number variation of the inner cylinder show that the fin arrangement has no significant effect on the heat transfer rate, and higher fin heights have a blocking effect on flow causing lower heat transfer rate. Kim and Ha [10] studied numerically laminar free convection inside annuli with internal fins. They found that the Nusselt number decreases with increasing the number of fins and the ratio of the annulus gap to inner radius. Ben-Nakhi and Chamkha [11] investigated effects of length and inclination of a thin fin placed on the middle of hot wall on free convection in a square cavity, using a numerical simulation. They found that the Rayleigh number, thin fin inclination and the fin's length have significant effects on the average Nusselt number of the heated wall of the cavity. The problem of free convection heat transfer in a tall cavity with adiabatic or heat conducting fins attached to one of the side walls was studied by Terekhov and Terekhov [12], numerically. They found that the mean Nusselt number for adiabatic fins, first increases with the number of fins to reach a maximum, and then decreases by approximately 30% compared to smooth walls. Ben-Nakhi and Chamkha [13] conducted a numerical simulation to study the conjugate free convection around a finned pipe in a square cavity with internal heat generation. They found that the finned pipe inclination angle, fins length, and the external and internal Rayleigh numbers have significant effects on the rate of heat transfer and flow field. Subsequently, Kasayapanand [14] investigated numerically free convection in a finned cavity under electric field. He found that the flow and heat transfer enhancements are the decreasing function of the Rayleigh number. Moreover, it is found that the heat transfer coefficient is substantially improved by the electric field effects, especially at the high number of fins, and the long fin length. Recently the problem of transition to a periodic flow in a differentially heated cavity with a thin fin on its side wall was investigated numerically by Xu *et al*. [15]. They found that the unstable temperature configuration above the fin results in intermittent plumes at the leeward side of the fin, which in turn, induce strong oscillations of the downstream boundary layer flow. Sharifi *et al*. [16] developed a numerical model for simulating the melting of a phase change material housed within an internally-finned metal enclosure and found that with horizontal fins, rapid melting occurred during the early stages of the phase change. Jani *et al.* [17] conducted a numerical simulation for study of laminar natural convection in a differentially heated square cavity with a high conductive thin fin on its cold wall. Their results showed that at high Rayleigh numbers, a long fin placed at the middle of the right wall had a more remarkable

effect on the flow field and heat transfer inside the cavity. An experimental and numerical study on laminar natural convection in a cavity heated from bottom due to an inclined fin was done by Varol *et al*. [18]. They observed that the heat transfer can be controlled by attaching an inclined fin on its wall.

In the present study, the problem of natural convection in an air filled square cavity heated from below and cooled from other walls, with a high conductive thin fin on its bottom wall is studied using the finite volume method. This problem may be occurred in a number of important technical applications such as enhancement and modification of cooling of electronic equipment and chips which has not been considered in the previous papers. In such a case, the electronic chip is located on the bottom of the cavity and the cold side walls are used to transfer the heat from the chip, while the fin attached on the bottom wall (chip) is used to increase the rate of heat transfer. The focus of the present study is to investigate the effects of the Rayleigh number and the length of the fin on temperature distribution, flow pattern and free convection characteristics inside this cavity.

Problem definition

A schematic view of the square cavity with a thin fin attached to its bottom wall considered in the present study is shown in fig. 1. The width and the height of the cavity are denoted by H. The length of the geometry perpendicular to its plane is assumed to be long enough; hence, the problem is considered two dimensional. The right and the left walls of the cavity, as well as its horizontal top wall are maintained at a constant temperature T_c, while its bottom wall is kept at a relatively high temperature T_h. A high conductive vertical thin fin is placed at the middle of the heated bottom wall, and is maintained at the same temperature of the wall to which it is attached. The dimensionless variable L for the length of the fin is defined as $L = l/H$. The fluid

Figure 1. A schematic diagram of the physical model

flow is assumed to be laminar and incompressible, and the thermophysical properties of air inside the cavity are assumed to be constant with the exception of the density which varies according the Boussinesq approximation [19].

The continuity, momentum, and energy equations for the 2-D, laminar, and steady free convection in a cavity are:

$$\frac{\partial u}{\partial x} + \frac{\partial v}{\partial y} = 0 \tag{1}$$

$$u\frac{\partial u}{\partial x} + v\frac{\partial u}{\partial y} = -\frac{1}{\rho}\frac{\partial p}{\partial x} + v\left(\frac{\partial^2 u}{\partial x^2} + \frac{\partial^2 u}{\partial y^2}\right) \tag{2}$$

$$u\frac{\partial v}{\partial x} + v\frac{\partial v}{\partial y} = -\frac{1}{\rho}\frac{\partial p}{\partial y} v\left(\frac{\partial^2 v}{\partial x^2} + \frac{\partial^2 v}{\partial y^2}\right) + g\beta(T - T_c) \tag{3}$$

$$u\frac{\partial T}{\partial x} + v\frac{\partial T}{\partial y} = \alpha\left(\frac{\partial^2 T}{\partial x^2} + \frac{\partial^2 T}{\partial y^2}\right) \tag{4}$$

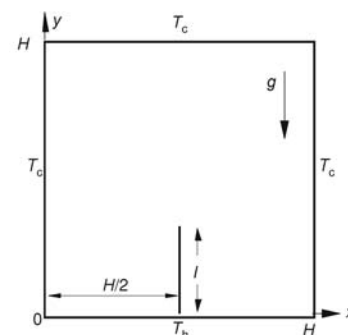Equations (1)-(4) can be converted to non-dimensional forms, using the following non-dimensional parameters:

$$X = \frac{x}{H}, Y = \frac{y}{H}, U = \frac{uH}{\alpha}, V = \frac{vH}{\alpha}, P = \frac{pH^2}{\rho\alpha^2}, \theta = \frac{T - T_c}{T_h - T_c} \tag{5}$$

The non-dimensional continuity, momentum and energy equations are:

$$\frac{\partial U}{\partial X} + \frac{\partial V}{\partial Y} = 0 \tag{6}$$

$$U\frac{\partial U}{\partial X} + V\frac{\partial U}{\partial Y} = -\frac{\partial P}{\partial X} + \Pr\left(\frac{\partial^2 U}{\partial X^2} + \frac{\partial^2 U}{\partial Y^2}\right) \tag{7}$$

$$U\frac{\partial V}{\partial X} + V\frac{\partial V}{\partial Y} = -\frac{\partial P}{\partial Y} + \Pr\left(\frac{\partial^2 V}{\partial X^2} + \frac{\partial^2 V}{\partial Y^2}\right) + \text{Ra}\,\Pr\,\theta \tag{8}$$

$$U\frac{\partial \theta}{\partial X} + V\frac{\partial \theta}{\partial Y} = \frac{\partial^2 \theta}{\partial X^2} + \frac{\partial^2 \theta}{\partial Y^2} \tag{9}$$

where the Rayleigh number and the Prandtl number, are:

$$\text{Ra} = \frac{g\beta\nabla T H^3}{\alpha\nu}, \quad \Pr = \frac{\nu}{\alpha} \tag{10}$$

The boundary conditions, used to solve the eqs. (6)-(9) are:

$$\begin{cases} \text{on cold walls} & U = V = 0, \quad \theta = 0 \\ \text{on cold walls and fin} & U = V = 0, \quad \theta = 1 \end{cases} \tag{11}$$

The stream function in dimensionless form is defined as:

$$U = \frac{\partial \Psi}{\partial Y}, \quad V = -\frac{\partial \Psi}{\partial X} \tag{12}$$

where

$$\Psi = \frac{\psi}{\alpha} \tag{13}$$

The local Nusselt number is defined as:

$$\text{Nu}_1 = \left|\frac{hH}{k}\right| \tag{14}$$

where h and k are heat transfer coefficient and thermal conductivity of the fluid (air), respectively. The heat transfer coefficient can be written as:

$$h = \frac{q_w}{T_h - T_c} \tag{15}$$

where

$$q_w = k\frac{\partial T}{\partial X} \quad \text{on vertical walls and} \quad q_w = k\frac{\partial T}{\partial Y} \quad \text{on horizontal walls} \tag{16}$$

By replacing eqs. (16) and (15) in eq. (14) the local Nusselt number along vertical and horizontal walls of the cavity can be written as:

$$\text{Nu}_1 = \left|\frac{\partial \theta}{\partial X}\right| \text{ on vertical walls} \tag{17}$$

and

$$\text{Nu}_1 = \left|\frac{\partial \theta}{\partial Y}\right| \text{ on horizontal walls} \tag{18}$$

The average Nusselt number of the cold wall $\mathrm{Nu_c}$, is obtained by integration of local Nusselt number along the cold walls:

$$\mathrm{Nu_c} = \frac{1}{3}\left\{ \int_0^1 \mathrm{Nu_1}\mathrm{d}Y \bigg|_{X=1} + \int_1^0 \mathrm{Nu_1}\mathrm{d}X \bigg|_{Y=1} + \int_1^0 \mathrm{Nu_1}\mathrm{d}Y \bigg|_{X=0} \right\} \tag{19}$$

The average Nusselt number of the hot wall and the fin, $\mathrm{Nu_{h,f}}$, is obtained by integration of local Nusselt number along the bottom wall and the fin length:

$$\mathrm{Nu_{h,f}} = \left\{ \int_0^1 \mathrm{Nu_1}\mathrm{d}X \bigg|_{Y=0} + \int_{\text{along the length of the fin}} \mathrm{Nu_1}\mathrm{d}Y \right\} \tag{20}$$

Also the average Nusselt number of the hot wall, $\mathrm{Nu_h}$, only is calculated to achieve a better understanding about the existence of the thin fin. This parameter is calculated according to:

$$\mathrm{Nu_h} = \int_0^1 \mathrm{Nu_1}\mathrm{d}Y \bigg|_{Y=0} \tag{21}$$

In order to study the effect of the fin on the average heat transfer rate for the hot and cold walls of the cavity, one may explained it via introducing a variable called the Nusselt number ratio (NNR) [8]:

$$\mathrm{NNR} = \frac{\mathrm{Nu}\big|_{\text{with a fin}}}{\mathrm{Nu}\big|_{\text{without a fin}}} \tag{22}$$

Thus, NNR for the cold walls, $\mathrm{NNR_c}$, for the hot wall, $\mathrm{NNR_h}$, and for the hot wall and the thin fin, $\mathrm{NNR_{h,f}}$, can be obtained according to eq. (22). Value of NNR greater than 1 indicates that the heat transfer rate is enhanced on that surface, whereas reduction of heat transfer is indicated when NNR is less than unity.

Numerical approach

The governing equations of mass, momentum, and energy, written in terms of the primitive variables are discretized using the finite volume method [20]. The coupling between velocity and pressure fields is done using the SIMPLER algorithm. The diffusion terms are discretized using a second-order central difference scheme; while, the hybrid scheme, which is a combination of first order upwind and first order central difference approximations, is employed to discretize the convective terms. The set of discretized equations are solved iteratively yielding values of the velocity, pressure, and temperature at the nodal points. An under-relaxation scheme is employed to obtain converged solutions. The convergence criterion is defined by the expression:

$$\text{Error} = \frac{\sum_{j=1}^{m}\sum_{i=1}^{n}\left|\xi^{t+1} - \xi^{t}\right|}{\sum_{j=1}^{m}\sum_{i=1}^{n}\left|\xi^{t+1}\right|} \le 10^{-7} \tag{23}$$

where *m* and *n* are the number of meshes in the x- and y- direction, respectively, ξ is the a transport quantity, and *t* – the number of iteration. It should be noted that finite discontinuities in temperature distribution appear at the edges of the bottom wall. In the present study this problem is resolved by assumption of the average temperature of the two walls at the corner nodes and keeping the adjacent nodes at their respective wall temperatures.

1124

Jani, S., *et al*: Numerical Investigation of Natural Convection Heat Transfer in ...
THERMAL SCIENCE: Year 2014, Vol. 18, No. 4, pp. 1119-1132

In order to validate the proposed numerical scheme, two different test cases are considered and the obtained results by the present code are compared with the existing results of these test cases in literature.

The first test case is laminar natural convection in an air-filled differentially-heated square cavity with a cold right wall, a hot left wall and adiabatic horizontal walls. The obtained results for this test case with the results of other investigates are presented in tab. 1. Also the percentages of difference between the results of the present study with those of other investigators are presented in this table.

As the second test case, the problem of natural convection in an air filled differentially-heated square cavity with a thin fin attached to its hot wall is analyzed, using the presented code, and the results are compared with the results of Shi and Khodadadi [8] for the same problem. The left and the right sidewalls of the cavity are maintained at constant temperatures T_h and T_c, respectively, with $T_h > T_c$; while, its top and bottom walls are insulated. The fin with the length of 0.35 of the width of the cavity is located in three different positions, namely, 0.25, 0.5, and 0.75 of the height of the hot wall. Figure 2 shows the streamlines for these cases at $Ra = 10^4$ obtained in the present study. Also the results of Shi and Khodadadi [8] for the same problem are presented in fig. 2. As it can be observed from tab. 1 and fig. 2 very good agreements exist between the obtained results of the present study and those obtained by other investigators.

Table 1. Comparison of the present results with those of other investigators for the natural convection in a differentially-heated square cavity filled with air

		Present study	Davis [21]	Markatos and Pericleous [22]	Fusegi *et al.* [23]
Nu	Ra = 10^3	1.113	1.118 (0.4%)	1.108 (0.45%)	1.105 (0.72%)
	Ra =10^4	2.254	2.243 (0.5%)	2.201 (2.3%)	2.302 (2%)
	Ra =10^5	4.507	4.519 (0.3%)	4.430 (1.7%)	4.646 (3.1%)
	Ra = 10^6	8.802	8.799 (0.03%)	8.754 (0.55%)	9.012 (2.4%)
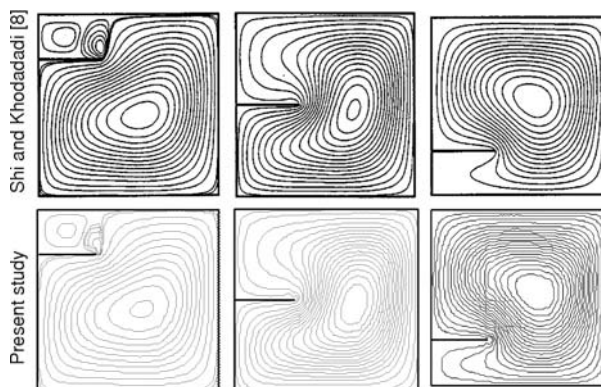
Figure 2. Comparison between the streamlines obtained by the present code and those of Shi and Khodadadi [8] for natural convection in a differentially heated square cavity with a horizontal thin fin on its hot wall ($Ra = 10^4$ and $Pr = 0.71$)

To conduct a grid independency study, an air filled cavity with a thin fin with the length of $L = 0.6$, attached to its bottom wall is considered, while the Rayleigh number is kept at $Ra = 10^6$. Six different uniform grids, namely, 21×21, 41×41, 61×61, 81×81, 101×101, and 121×121 are employed for the numerical simulations. The average Nusselt numbers of the cold walls of the cavity correspond to these grids are shown in tab. 2. Based on the results of this fig-

ures, a 61×61 uniform grid is used for all of the subsequent numerical calculations. Percentages of difference of the average Nusselt number for all grids compared to 61×61 grid are presented in this table.

Table 2. Average Nusselt number of cold walls for different uniform grids

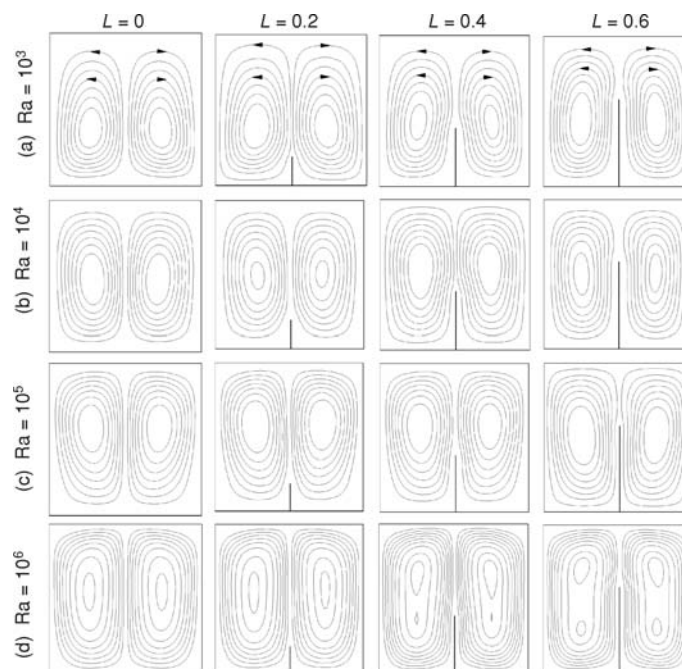| Grid size	21×21	41×41	61×61	81×81	101×101	121×121
Nu	6.011 (19%)	7.212 (3.65%)	7.486	7.487 (0.01%)	7.488 (0.02%)	7.488 (0.03%)

Results and discussion

Having verified the numerical procedure via solving different test cases and comparing the results with the existing results in the literature, the proposed code is employed to investigate the problem of the natural convection fluid flow and heat transfer inside the air filled square cavity with a vertical thin fin attached to the middle of its bottom wall, shown in fig.1. The Prandtl number of the air is kept at 0.71. The effects of the fin's length, L, and the Rayleigh number, on the change of the absolute values of Ψ_{max} (maximum value of the stream function field) will be shown and analyzed. Furthermore, representative results for the local and average Nusselt number and the NNR for various conditions will be presented and discussed. The results are presented for a range of Rayleigh numbers from 10^3 to 10^6, and four length of the fin, namely, 0, 0.2, 0.4, and 0.6.

Figure 3 presents the variation of streamlines inside a square cavity with respect to the Rayleigh number and different lengths of the fin. Some arrows indicating rotation of vortices are shown in the figure at Ra = 10^3. As it seen from this figure, due to the symmetrical geometry and boundary conditions on the walls, the flow consists of two counter rotating vortices which are fairly symmetric, regardless of the fin's length and the Rayleigh number. For all values of L, as the Rayleigh number increases, the kernel of each vortex moves upward and the streamlines become more packed next to the fin and the walls of the cavity, implying that the flow moves faster as free convection is intensified. It is observed that for Ra ≤ 10^5, the kernel of each vortex moves upward somewhat by increasing the fin's length up to 0.4, but then moves downward for the case of $L = 0.6$. At

Figure 3. Streamlines for different length of the fin and various Rayleigh numbers

Jani, S., *et al*: Numerical Investigation of Natural Convection Heat Transfer in ...

1126   THERMAL SCIENCE: Year 2014, Vol. 18, No. 4, pp. 1119-1132

$Ra = 10^6$, the kernel of each vortex breaks into two distinct smaller vortices for large values of L (0.4 and 0.6). This behavior can be related to the stronger buoyant flows at this Rayleigh number which intensify the strength of the circulating vortices which affects the formation of the inner eddies.

Figure 4 shows variation of the absolute value of stream function with the length of the fin, for different Rayleigh numbers from 10^3 to 10^6, respectively. It should be noted that for a differentially heated square cavity as the Rayleigh number increases the difference between the values of stream function on the wall (generally taken to be zero) and the extreme values of the stream function field (minimum or maximum) widens monotonously. Therefore, the absolute value of Ψ_{max} (maximum value of the stream function field) can be viewed as a measure of the intensity of natural convection. So it is necessary to study how the length of the fin affects the absolute value of the Ψ_{max}. It is evident from the figure that the variations range of Ψ_{max} for each Rayleigh number, increases by increasing the Rayleigh number which causes stronger buoyant forces, figs. 4(a)-4(d). For $Ra = 10^3$, fig. 4(a), the absolute value of Ψ_{max} increases with increasing L, for all considered values of lengths of the fin. At $Ra = 10^3$, where conduction dominates the heat transfer regime, an increase in the fin's length intensities the natural convection which results an enhancement in the strength of the vortices somewhat.
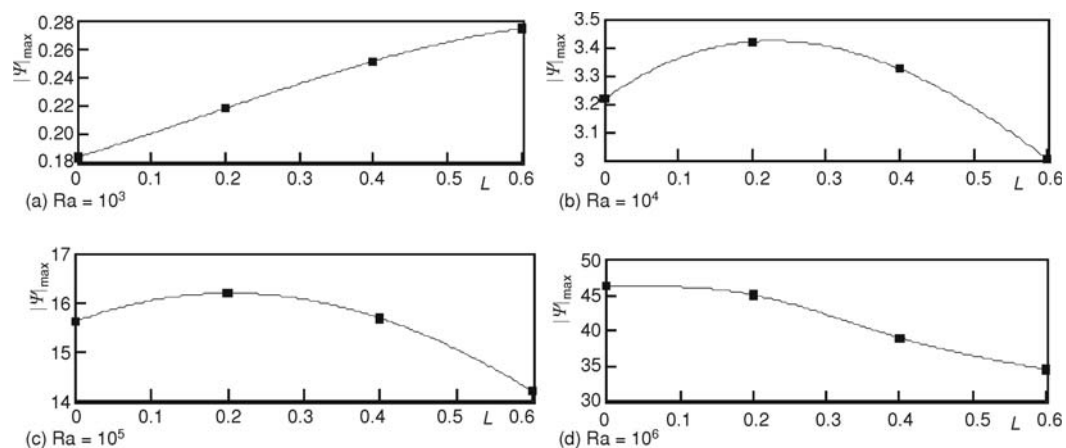

Figure 4. Variation of the absolute value of Ψ_{max} with the length of the fin

For $Ra = 10^4$, fig. 4(b), placing a fin at the middle of the bottom wall with $L \leq 0.4$ can enhance the main vortices, but for $0.4 \leq L \leq 0.6$ it can weaken the main vortices. Noting that although the absolute value of Ψ_{max} decreases for $L > 0.2$, but is still larger than that of the no-fin case ($L = 0$), in the range of $L = 0.2$ to 0.4. Hence, while the fin's length is shorter than 0.4, placing a fin at the bottom of the cavity intensifies the circulating cells in comparison with a no-fin cavity, for $Ra = 10^4$. For $L > 0.45$, the fin's presence brings about resistance to the motion of the vortexes and weakens the intensity of them. From another point of view, it can be said that for $L < 0.2$ the extra heating effect of the fin is dominant which increases the flow strength. As the fin becomes longer, the friction loss of the fin increases which decreases the strength of the fluid flow. The same manner for the absolute values of Ψ_{max} can be observed for the case of $Ra = 10^5$, fig. 4(c). Similar to the case of $Ra = 10^4$, the fluid flow weakens for the high values of the fin's length ($L > 0.4$). Figure 4(d) shows the variation of the absolute value of Ψ_{max} with the length of

the fin when Ra = 10^6. Due to this figure, one can observe that all the computed Ψ_{max} values are below the value of the no-fin case ($L = 0$). This means that the presence of a fin of any length can always decrease the strength of the two counter-rotating vortices. This reduction is because the hot fin's effect of resisting the fluid motion is more dominant than the effect of heating the fluid to enhance the two circulating cells in this case.

In summary, one can observe that most computed absolute values of Ψ_{max} are greater than those with no fin for the low and moderate Rayleigh numbers, namely Ra = 10^3, 10^4, and 10^5, whereas all computed absolute values of Ψ_{max} are smaller than those with no fin at Ra = 10^6. This implies that the extra heating effect of the hot fin and enhancing the strength of two counter-rotating vortices becomes less marked with the rise of the Rayleigh number, while friction loss and resistance effect of the fin on the motion of the vortices becomes more important.

Figure 5 depicts the isotherm contours in a square cavity with a vertical thin fin attached to middle of its bottom wall for various Rayleigh numbers, and for different lengths of the fin ($L = 0$, 0.2, 0.4, and 0.6). The isotherms also have symmetrical shape at each Rayleigh number however, they display different behaviors as the Rayleigh number changes. For the cases of Ra = 10^3 and 10^4, where conduction dominates the heat transfer regime, the variation of
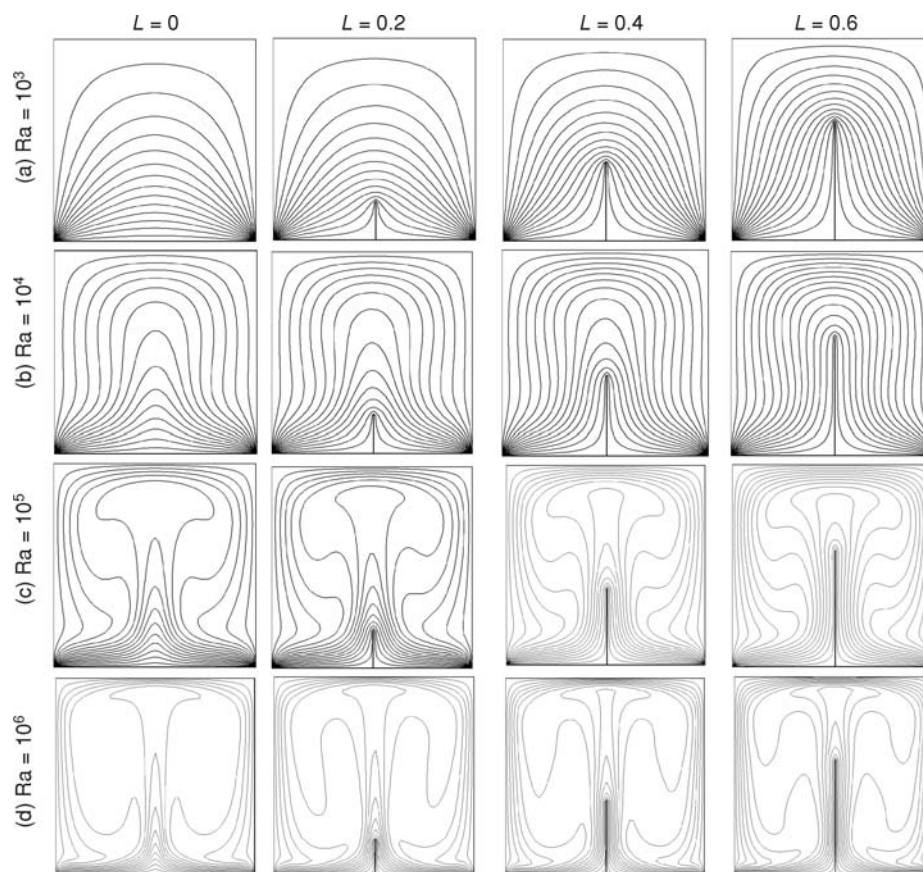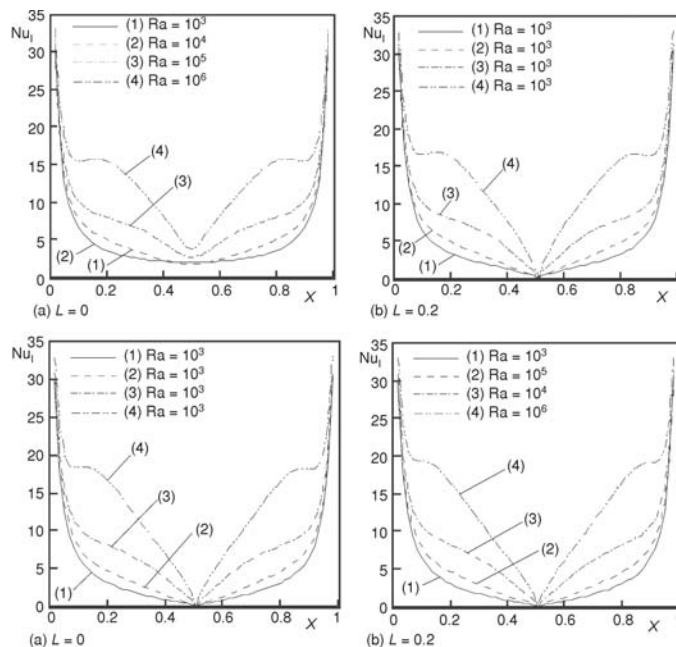

Figure 5. Isotherms for different length of the fin and various Rayleigh numbers

Jani, S., *et al*: Numerical Investigation of Natural Convection Heat Transfer in ...

1128   THERMAL SCIENCE: Year 2014, Vol. 18, No. 4, pp. 1119-1132

the fin's length only changes the temperature distribution locally at the vicinity of the thin fin and the rest of the cavity remains nearly unaffected. For each length of the fin, it can be seen that by increase in the Rayleigh number, the isotherms in the vicinity of the fin and next to the walls of the cavity becomes more densely packed. This phenomenon is the major characteristic of natural convection heat transfer. Moreover, with increasing the Rayleigh number, as the streamlines exhibit stronger flow patterns, the isotherms display more distinguished boundary layers. In addition, one can observed the thermal stratification in the regions between the fin and the sidewalls of the cavity, which is more pronounced for the higher values of L.

A plume-like temperature distribution is also obtained near the top wall of the cavity which becomes more noticeable by increasing the fin's length. The convection region adjacent to the fin and the sidewalls of the cavity becomes thinner and more packed, producing higher temperature gradients, with increasing Rayleigh number.

The variation of the local Nusselt number, Nu_l, along the bottom wall of the cavity, for the Rayleigh number ranging from 10^3 to 10^6, and for different lengths of the fin ($L = 0, 0.2, 0.4$, and 0.6) is illustrated in figs. 6(a)-6(d), respectively. It can be seen that the variation of the local Nusselt number along the heated wall is symmetric and nearly identical for each Rayleigh number, regardless of the fin's length. The local Nusselt number increases by increase in the Rayleigh number, while the deviation of local Nusselt number for different values of Rayleigh number increases by moving far from the fin's location. This is because as the Rayleigh number increases, the heat transfer rate within the cavity intensifies and consequently, causes an increase in the variation slope of local Nusselt number along the bottom wall. As can be seen from the figure no heat transfer occurs from the bottom wall in the regions close to the fin's location ($X \rightarrow 0.5$), because of the presence of a tiny dead zone next to a corner region between the bases of the fin and the bottom wall of the cavity. Also 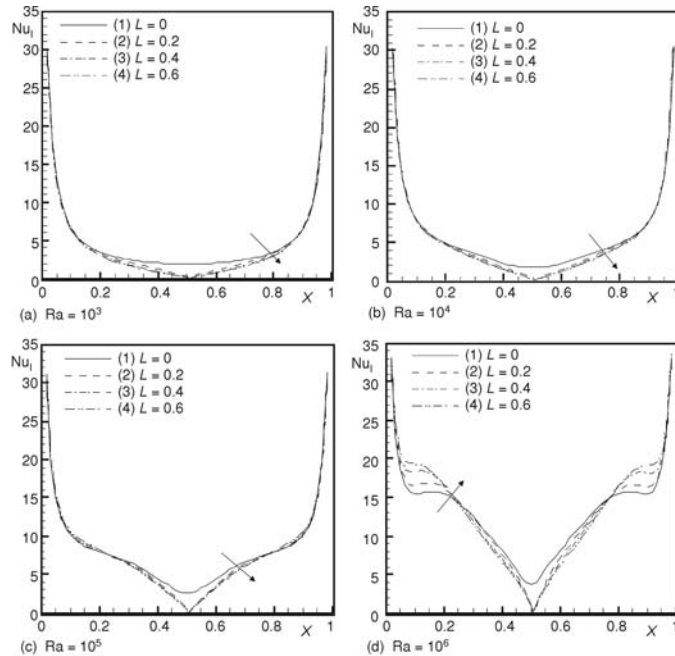it is evident that at the vicinity of the side walls, which a steep temperature gradient exists, for all values of Rayleigh number, the same local Nusselt numbers are obtained.

The effect of the length of the fin on the local Nusselt number, along the bottom wall of the cavity is depicted in figs. 7(a)-(d), for different Rayleigh numbers. It is evident that in the presence of a fin, the value of local Nusselt number exhibits a sharp reduction at the location of the wall/fin intersection where it becomes a minimum there due to flow stagnation. In principle, the attachment of a fin in the middle of the heated bottom wall always reduces the local Nusselt number for the heated wall by a ratio that is re-
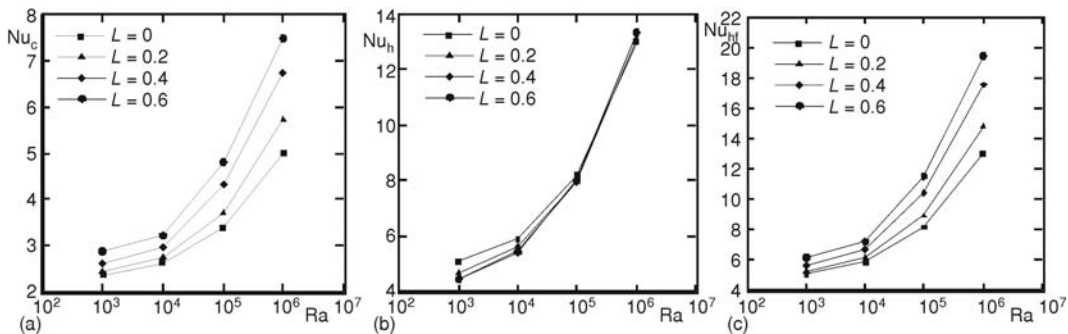

Figure 6. Variation of the local Nusselt number along the bottom wall of the cavity with Rayleigh number

lated to *L* and Rayleigh number. For the cases with Ra= $= 10^3$, 10^4, and 10^5, the local Nusselt number of the bottom wall exhibits insensitivity to the length of the fin when a hot fin is placed near the middle of the bottom wall. For Ra $= 10^6$, and in the medial regions of the bottom wall ($0.25 < X < 0.75$), one can observed that the local Nusselt number of the bottom wall decreases somewhat with an increase in the length of the fin, whereas in the regions close to the both ends of the bottom wall, the maximum values of local Nusselt number are related to the longer fin lengths. This behavior can be due to the stronger buoyant flows in the regions far from the position of the fin, at this Rayleigh number. It was previously observed

Figure 7. Variation of the local Nusselt number along the bottom wall of the cavity with fins at different lengths

that at Ra $= 10^6$ via existence of a thin and its friction loss effect, the flow intensity decreases for all length of the fin. Therefore at this Rayleigh number, the local Nusselt number along the bottom wall at the vicinity of the fin decreases with increase in the fin's length, whereas in the regions close to the side wall, which the friction loss effects of the fin weaken, the local heat transfer increase with increase in the fin's length.

Figures 8(a)-(c) show the effect of the length of the fin on the average Nusselt number of the cold walls, hot wall, and the hot wall with the thin fin, at different Rayleigh numbers, respectively. It may be noted that with a fin placed on the middle of the hot wall, the difference between the average Nusselt numbers of the cold walls and the hot wall only signifies the enhanc-

Figure 8. Variation of the average Nusselt number along the cold and hot walls of the cavity with respect to Rayleigh number and for fin at different lengths; (a) cold walls, (b) hot wall, and (c) hot wall and thin fin

Jani, S., *et al*: Numerical Investigation of Natural Convection Heat Transfer in ...

1130   THERMAL SCIENCE: Year 2014, Vol. 18, No. 4, pp. 1119-1132

ing or degrading role of the fin in transferring heat from the hot wall to the cold walls. Also, a comparison between the average Nusselt numbers of the hot wall only, and the hot wall and the thin fin together can show the heat transfer from the fin. From these figures, it can be seen that the average Nusselt numbers for the cold walls (Nu_c), the hot wall (Nu_h), and the hot wall and the thin fin ($Nu_{h,f}$), increase with the rise of the Rayleigh number, regardless of the fin's length. It should be noticed that the average Nusselt number increases on the cold walls and the hot wall with thin fin with increase in the length of the fin, regardless the Rayleigh number, whereas decreases somewhat on the hot wall with the rise of the fin's length, especially for the lower values of Rayleigh number, *i. e.*, $Ra \leq 10^4$. This is because for the average Nusselt number on the cold walls and the average Nusselt number of the hot wall with the thin fin, as the length of the fin increases, the effect of the extra heating of the fin and enhancing the main vortex becomes more remarkable in comparison with the resistance effect of the fin on the movement of the vortices, with the rise of the Rayleigh number. For the case of the average Nusselt number along the hot wall only, these two mechanisms certainly counter balance each other at the higher Rayleigh numbers, namely, $Ra = 10^5$ and 10^6. Finally, it can be concluded that when a thin fin is located at the middle of the bottom wall, the total heat transferred to the fluid increases, while the rate of heat transfer from only the hot wall decreases. Therefore, this further heat transfer to the fluid is due to the thin fin.

Figures 9(a)-(c) show the variations of NNR for the cold walls, NNR_c, hot wall, NNR_h, and the hot wall with the thin fin, $NNR_{h,f,}$ with the fin's length for different values of Rayleigh number. Based on these figures, it is observed that placing a fin on the middle of the bottom wall always increases heat transfer on the cold walls, since NNR_c is always more than 1. Moreover, it is to be noticed in these figures that the average Nusselt number for the cold walls and the hot wall with the thin fin becomes larger with the increase of the fin's length, regardless of the Rayleigh number fig. 9(a) and 9(c). This is because the extra heating of the fin near the fin which enhances the corresponding convection in that area, especially at the higher values of Rayleigh number, which this effect becomes more noticeable. The heat transfer rate on the only hot wall always reduces for any length of the fin, in lower Rayleigh numbers ($Ra = 10^3$ and 10^4), but increases for the higher Rayleigh numbers ($Ra = 10^5$ and 10^6) somewhat fig. 9(b). These trends are similar to those were presented in fig. 8(b). Thus, similar discussions can be extended. Due to fig. 9(b), it can be observed that the average Nusselt number of the heated wall exhibits nearly insensitivity to the length of the fin if $L \geq 0.2$.
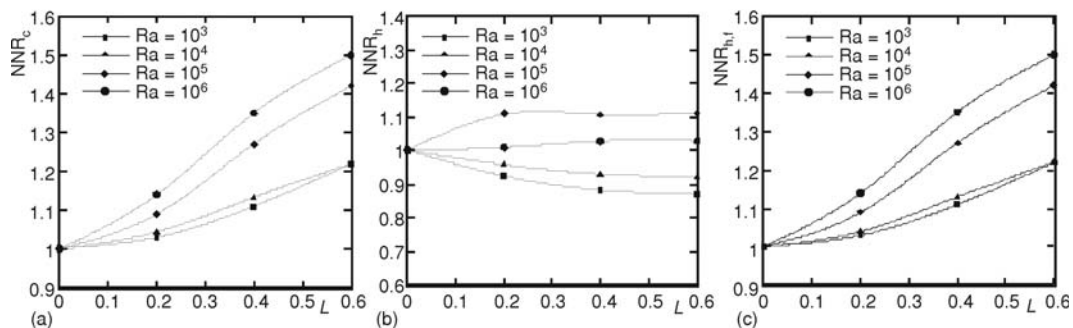

Figure 9. Variation of NNR along the cold and hot walls of the cavity with fins at different lengths; (a) cold walls, (b) hot wall, and (c) hot wall and thin fin

Jani, S., *et al*: Numerical Investigation of Natural Convection Heat Transfer in ...
THERMAL SCIENCE: Year 2014, Vol. 18, No. 4, pp. 1119-1132

1131

Conclusions

Using the finite volume method, the free convection fluid flow and heat transfer inside a symmetrically-cooled square cavity with a fin attached to its heated bottom wall was studied numerically and the following results were obtained.

- For all considered values of the Rayleigh number and length of the fin, two fully developed counter-rotating vortices are formed inside the cavity.
- Two different effects for the thin fin are identified. The first is extra heating of the fin which increases the rate of heat transfer and intensifies the natural convection. The second is the friction loss of the fin which weakens the fluid flow within the cavity and decreases the rate of heat transfer.
- At $Ra = 10^3$, the flow strength increases with increasing the length of the fin while at $Ra = 10^4$ and 10^5 it occurs for $L < 0.4$ and further increase in the length of the fin decreases the flow strength. At $Ra = 10^6$, nearly pure convection regime, the existence of the fin with all lengths reduces the flow strength.
- Existence of a thin fin at middle of the bottom wall motivates the fluid flow to be blocked in this region follows reduction of the local Nusselt number in regions adjacent to middle of the bottom wall.
- By placing a thin fin on the middle of the bottom wall the average Nusselt number of the cold walls increases and as the Rayleigh number increases, the favorite effect raises.
- By placing a thin fin on the bottom wall of the cavity the total heat transferred to the fluid inside the cavity increases, while the average Nusselt number of only the bottom wall decreases. Therefore the further heat transfer occurs due to the thin fin.

Nomenclature

g – gravitational acceleration, [ms^{-2}]
H – height and width of cavity, [m]
h – heat transfer coefficient, [Wm^{-2}K^{-1}]
k – thermal conductivity, [Wm^{-1}K^{-1}]
L – dimensionless length of the fin
l – length of the fin, [m]
NNR – Nusselt number ratio
Nu – average Nusselt number
Nu_l – local Nusselt number
P – dimensionless pressure
p – pressure, [Nm^{-2}]
Pr – Prandtl number
q_w – heat flux, [Wm^{-2}]
Ra – Rayleigh number
T – temperature, [K]
U, V – velocities components in X- and Y-direction
u, v – dimensional velocities components in x- and y-direction, [ms^{-1}]

X, Y – dimensionless Cartesian co-ordinates
x, y – Cartesian co-ordinates, [m]

Greek symbols

α – thermal diffusivity, [m^{2}s]
β – thermal expansion coefficient, [K^{-1}]
θ – dimensionless temperature
ν – kinematic viscosity, [m^{2}s^{-1}]
r – density, [kgm^{-3}]
Ψ – dimensionless stream function
ψ – stream function, [m^{2}s^{-1}]

Subscripts

c – cold wall
h – hot wall
h, f – hot wall and fin
l – local

References

[1] Ostrach, S., Natural Convection in Enclosures, *ASME J. Heat Trans., 110* (1988), 4b, pp. 1175-1190
[2] Zimmerman, E., Acharya, S., Natural Convection in an Enclosure with a Vertical Baffle, *Commun. Appl. Numer. Meth., 4* (1988), 5, pp. 314-338
[3] Frederick, R. L., Natural Convection in an Inclined Square Enclosure with a Partition Attached to its Cold Wall, *Int. J. Heat and Mass Trans., 32* (1989), 1, pp. 87-94

1132

Jani, S., *et al*: Numerical Investigation of Natural Convection Heat Transfer in ...
THERMAL SCIENCE: Year 2014, Vol. 18, No. 4, pp. 1119-1132

[4] Frederick, R. L., Valencia, A., Heat Transfer in a Square Cavity with a Conducting Partition on its Hot Wall, *Int. Commun. Heat and Mass Trans., 16* (1989), 3, pp. 347-354

[5] Nag, A., *et al*., Natural Convection in a Differentially Heated Square Cavity with a Horizontal Partition Plate on the Hot Wall, Comput. *Methods Appl. Mech. Eng., 110* (1993), 1-2, pp. 143-156

[6] Lakhal, E. K., *et al*., Natural Convection in Inclined Rectangular Enclosures with Perfectly Conducting Fins Attached on the Heated Wall, *Heat Mass Transfer, 32* (1997), 5, pp. 365-373

[7] Bilgen, E., Natural Convection in Enclosures with Partial Partitions, *Renewable Energy, 26* (2002), 2, pp. 257-270

[8] Shi, X., Khodadadi, J. M., Laminar Natural Convection Heat Transfer in a Differentially Heated Square Cavity Due to a Thin Fin on the Hot Wall, *ASME J. Heat Trans., 125* (2003), 4, pp. 624-634

[9] Rahnama, M., Farhadi, M., Effect of Radial Fins on Two-Dimensional Turbulent Natural Convection in a Horizontal Annulus, *Int. J. Therm. Sci., 43* (2004), 3, pp. 255-264

[10] Kim, M., Ha, J., Numerical Simulation of Natural Convection in Annuli with Internal Fins, *KSME Int. J., 18* (2004), 4, pp. 718-730

[11] Ben-Nakhi, A., Chamkha, A. J., Effect of Length and Inclination of a Thin Fin on Natural Convection in a Square Enclosure, *Numer. Heat Trans.-Part A, 50* (2006), 4, pp. 381-399

[12] Terekhov, V. I., Terekhov, V. V., Heat Transfer in a High Vertical Enclosure with Fins Attached to One of the Side Walls, *High Temp., 44* (2006), 3, pp. 436-44

[13] Ben-Nakhi, A., Chamkha, A. J., Conjugate Natural Convection around a Finned Pipe in a Square Enclosure with Internal Heat Generation, *Int. J. Heat and Mass Trans., 50* (2007), 11, pp. 2260-2271

[14] Kasayapanand, N., A Computational Fluid Dynamics Modeling of Natural Convection in Finned Enclosure under Electric Field, *Appl. Therm. Eng., 29* (2009), 1, pp. 131-141

[15] Xu, F., *et al*., Transition to a Periodic Flow Induced by a Thin Fin on the Sidewall of a Differentially Heated Cavity, *Int. J. Heat Mass Trans., 52* (2009), 3-4, pp. 620-628

[16] Sharifi, N., *et al*., Enhancement of PCM Melting in Enclosures with Horizontally-Finned Internal Surfaces, *Int. J. Heat Mass Trans., 54* (2011), 19-20, pp. 4182-4192

[17] Jani, S., *et al*., Numerical Study of Free Convection Heat Transfer in a Square Cavity with a Fin Attached to Its Cold Wall, *Heat Transfer Research, 42* (2011), 3, pp. 251-266

[18] Varol, Y., *et al*., Experimental and Numerical Study on Laminar Natural Convection in a Cavity Heated from Bottom Due to an Inclined Fin, *Heat Mass Transfer, 48* (2012), 1, pp. 61-70

[19] Bejan, A., *Convection heat Transfer*, John Wiley & Sons Inc., New York, N. J., 2004

[20]   Patankar, S. V., Numerical Heat Transfer and Fluid Flow, Hemisphere Publishing Corporation, Taylor and Francis Group, New York, USA, 1980

[21] Davis G. V., Natural Convection of Air in a Square Cavity, a Benchmark Numerical Solution, *Int. J. Numer. Methods fluids, 3* (1983), pp. 249-264

[22] Markatos N. C., Pericleousl, K.A., Laminar and Turbulent Natural Convection an Enclosed Cavity, *Int. J. Heat Mass Tran., 27* (1984), 5, pp. 772-775

[23] Fusegi, T., *et al*., A Numerical Study of Tree-Dimensional Natural Convection in a Differentially Heated Cubical Enclosure, *Int. J. Heat Mass Tran. 34* (1991), 6, pp. 1543-1557